Chapter 1
O_2-Sensitive Probes Based on Phosphorescent Metalloporphyrins

Ruslan I. Dmitriev and Dmitri B. Papkovsky

Abstract Measurement of molecular O_2 in biological samples represents an important group of analytical methods actively employed in diverse areas of biology (microbes, plants, animals), medicine and toxicology. In this chapter, the significance, classification of main methods and principles of quenched-phosphorescence measurements of O_2 with the help of metalloporphyrin based probes are described. Various measurement platforms are discussed with particular attention to the experimental models.

Keywords Oxygen-sensitive probes · Pt-porphyrins · Phosphorescence quenching · Time-resolved fluorescence · Intracellular probes · Oxygen sensing and imaging · In vitro assays · Cellular oxygen

1.1 Introduction

Measurement of molecular oxygen (O_2) in biological samples containing respiring cells and tissues is of high practical and biomedical importance. O_2 is a small, gaseous, non-polar analyte which has moderate solubility in aqueous media ($\sim$200 μM at air saturation, 37 °C). It is supplied to cells and tissues by passive diffusion and, in higher multicellular organisms, by convectional transport via vasculature, red blood cells and haemoglobin [1, 2]. In mammalian cells O_2 is the key metabolite and the source of energy involved in the production of ATP through the electron transport chain and oxidative phosphorylation [3]. It is a substrate of numerous enzymatic reactions vital for cellular function, involved in cell signalling and genetic adaptation to hypoxia [4, 5]. Therefore, detailed understanding of biological roles of O_2 is of fundamental importance for cell biology, medicine, drug discovery and other disciplines [1, 6].

D. B. Papkovsky et al., *Phosphorescent Oxygen-Sensitive Probes*,
SpringerBriefs in Biochemistry and Molecular Biology,
DOI: 10.1007/978-3-0348-0525-4_1, © The Author(s) 2012

The main analytical tasks in O_2 measurement are: (1) assessment of bulk oxygenation of samples containing cells, tissues, organs and whole organisms; (2) measurement of O_2 consumption rates (OCR); (3) analysis of O_2 distribution, localised gradients and O_2 maps in heterogeneous samples; (4) analysis of subcellular O_2 gradients, and (5) monitoring of dynamics of parameters 1–4 in response to changes in cellular function, for example, in normal/resting and diseased/stimulated cells and tissues.

Analytical task 1 probably has the highest importance: under normal physiological conditions, O_2 levels in different tissues are maintained within the defined limits, which are tissue-specific [7, 8]. Significant alterations in oxygenation from the norm are observed in diseased tissues and under pathological conditions, e.g. in solid tumours, under ischaemia/stroke, anaemia, neurodegeneration, hypertension, metabolic disorders. Short-term and sustained hypoxia can lead to cell death or protection and adaptive responses via rearrangement of cell metabolism. The latter includes Warburg effect, hypoxia-induced expression of regulatory genes and proteins such as HIF-1α, PGC-1α [2, 5, 9–11] and their downstream products. On the other hand, significant spatial and temporal fluctuations in O_2 occur in exercised skeletal and cardiac muscles, excited regions of the brain, kidney during their normal function [2, 12–14].

OCR reflects respiratory activity of a sample and, together with other biomarkers such as ATP content, mitochondrial membrane potential, metabolite concentrations and ion fluxes, provides important information on the metabolic activity and bioenergetic status. Significant alterations in cellular OCR reflect perturbed metabolism, mitochondrial dysfunction, disease state or drug toxicity [3]. Analytical tasks 3–5 are best addressed by means of O_2 imaging techniques, which allow mapping of O_2 concentration within biological samples in 2D, 3D and 4D (time lapse experiments), and with sub-micrometer spatial resolution.

Due to the high importance of O_2 measurement, the diversity of analytical tasks and biological objects to be analysed, different measurement methodologies have been developed for O_2 sensing. The particular sample, measurement location, concentration range, sampling frequency and resolution of O_2 to be measured determine the choice of experimental technique, measurement format, detection modality, the particular probe, instrumentation and other tools.

Among these the following main groups can be defined:

1. Electrochemical methods utilising electrodes, such as the Clark electrode system.
2. Physical methods utilising paramagnetic properties of O_2, such as EPR spectrometry.
3. Optical methods.

The Clark-type electrode [15] has a relatively simple set-up and low cost. In this system, sample O_2 diffuses through a Teflon membrane to a Pt electrode polarised at about +0.7 V against the Ag/AgCl electrode, where it gets reduced generating current proportional to O_2 concentration. Its main applications are point measurement of dissolved O_2 and absolute OCR of macroscopic biological

samples containing suspension cells or isolated mitochondria in a sealed, stirred and temperature controlled cuvette, as well as measurement of local O_2 levels in cells and tissues with microelectrodes [16, 17]. Their principal drawbacks are O_2 consumption by the electrode itself, the need for stirring and regular maintenance, baseline drift, poisoning and fouling of the electrode, poor compatibility with adherent cells and effector treatments, limited throughput. In the past years, much progress has been made in addressing these limitations and adapting the technology for use with adherent cell lines in multiparametric biochips [16] or customised systems for cerebellar granule neurons [17, 18].

Electron paramagnetic resonance (EPR) is a physical method for detecting molecules with unpaired electrons. Since O_2 is a paramagnetic molecule, EPR can be used for its quantification, directly or indirectly using dedicated probes. Extracellular EPR probes such as India Ink [19] were developed for clinical use and assessment of cell populations. Nitroxyl and esterified trityl radicals (e.g. triarylmethyl) represent promising probes for EPR imaging of intracellular O_2 [20, 21]. In vivo EPR imaging with micron resolution ($30 \times 30 \times 100$ μm) has been demonstrated [22] which complements the other O_2 sensing techniques well. EPR spectra and intensity signals can be used for quantification.

Optical methods rely on endogenous or exogenous probes which alter their properties in response to fluctuations in O_2 concentration. The absorption-based methods (e.g. myoglobin in muscle tissue [23]) have been complemented by the luminescence-based techniques which include the measurement of fluorescence of redox indicators (e.g. NADH and FAD) [24], delayed fluorescence of endogenous protoporphyrin IX [25, 26], photoacoustic tissue imaging [27], GFP-based biosensor constructs [28–30] and quenched-luminescence O_2 sensing [31–33].

Luminescence quenching represents one of the most powerful and versatile techniques which allows direct, minimally or non-invasive, real-time monitoring and imaging of O_2 in biological samples with good selectivity and tunable sensitivity [32, 34]. This technology provides reliable and accurate detection of O_2 in different formats including single point macroscopic sensors and microsensors, in vitro bioassays based on O_2 detection, screening platforms (cell, enzyme and animal based) operating on commercial fluorescent readers, sophisticated live cell and in vivo imaging systems, multi-parametric systems in which O_2 detection is coupled with the other probes and biomarkers. A number of such systems and applications have already gained wide use and are produced commercially [35, 36].

The key components of the optical O_2 sensing technique are dedicated luminescent materials that enable O_2 to be probed in complex biological objects, particularly those containing respiring cells. The main O_2 pools that require quantification and monitoring are: (i) dissolved extracellular O_2 in growth medium or vasculature; (ii) pericellular O_2 in the interstitial space, at cell surface; (iii) intracellular O_2 in the cytosol, mitochondria or other compartments; (iv) in vivo measurement of O_2 distribution in live tissues, organs and whole organisms.

Pt(II)- and Pd(II)-porphyrins and some related structures possessing strong phosphorescence at room temperature, moderate quenchability by O_2 and high chemical stability are among the common indicator dyes used in O_2-sensing

materials [32, 37]. Fluorescent complexes of Ru(II), Os(II), Ir(III)-porphyrins, lanthanide chelates are also being actively explored in O_2 sensor chemistries [38–40], however, they are outside the scope of this book. In this chapter, we will focus on the general principles of quenched-luminescence detection of O_2, main types of sensor materials on the basis of phosphorescent porphyrin dyes, different measurement formats of O_2 sensing technique and detection modalities and their core application in conjunction with various biological models.

1.2 Principles of Quenched-Phosphorescence Detection of O_2

Molecular O_2 is an efficient quencher of long-lived excited triplet states which acts via collisional interaction with luminophore molecules causing their radiationless deactivation and return to the ground state. In the presence of O_2 phosphorescence intensity (I) and lifetime (τ) are both reduced, the relationship between measured luminescent parameter and O_2 concentration is described by the Stern–Volmer equation [41]:

$$I_0/I = \tau_0/\tau = 1 + K_{s-v*}[O_2] = 1 + k_{q*}\tau_{0*}[O_2], \quad (1.1)$$

where I_0 and τ_0 are unquenched intensity and lifetime at zero O_2, respectively, K_{s-v} is the Stern–Volmer quenching constant, and k_q—the bimolecular quenching rate constant, which depends on the immediate environment of the reporter dye, temperature and sterical factors. Each luminescent material has a characteristic relationship between $[O_2]$ and τ (or I). Luminescence lifetime represents the average time which the luminophore stays in the excited state before emitting a photon. This is an intrinsic feature of the material independent on the dye concentration and measurement set-up. For this reason, lifetime is a preferred measurement parameter for O_2 quantification by luminescence quenching. Microsecond range lifetimes of the phosphorescent dyes are relatively easy to measure, unlike the nanosecond lifetimes of conventional fluorophores which require short excitation pulses and high speed detectors [42]. By conducting phosphorescence lifetime or intensity measurements with the sensor, O_2 concentration within test sample can be quantified as follows:

$$[O_2] = (\tau_0 - \tau)/(\tau_* K_{s-v}) \quad (1.2)$$

Equations 1.1 and 1.2 are only valid for homogeneous populations of dye molecules in quenching medium, such as solution-based systems, producing linear Stern–Volmer relationship of $[O_2]$ versus τ^{-1} and allowing simple two-point calibration. However, many of the existing O_2-sensitive materials exhibit pronounced heterogeneity which results in nonlinear Stern–Volmer relationship [43]. This should be considered in the mechanistic description (physical model) and experimental calibration of the sensor. Calibration usually involves measurement

of sensor signal (τ or I) at several known O_2 concentrations (standards) under constant temperature (25–37 °C for biological objects), and fitting these data points to determine the function $[O_2] = f(\tau,I)$. Under equilibrium, the concentration of O_2 in solution (and within the sensor material) is related to the partial pressure of O_2 in the gas phase, according to Henry's law. Sensor calibration in lifetime scale, i.e. $[O_2] = f(\tau)$, can be regarded as absolute, and indeed there are some commercial O_2 sensor systems which operate with factory calibration [35]. However, blind application of the available calibration on a different instrument, measurement set-up or sample type imposes a risk of generating inaccurate O_2 values. For proper operation of the sensor and accurate determination of O_2 concentration without significant instrumental errors and measurement artefacts, periodic re-calibrations or at least once-off independent calibrations should be considered.

Among the common sources of errors in O_2 measurement, is variation of sample/sensor temperature during the measurement. Since most of the O_2 sensors display strong temperature dependence of calibration, temperature drift or instability can skew the results of O_2 measurement. Singlet oxygen, a by-product of the quenching process and highly reactive but rather short-lived form of O_2, is another cause of concern. Produced by photosensitisation, singlet oxygen mostly returns back to the ground state O_2. But it can also react with nearby molecules (dye, lipids, proteins, nucleic acids) and damage the sensor or biological sample and affect the measurements [44].

1.3 Phosphorescent Metalloporphyrins and O_2-Sensitive Materials on Their Basis

Within the group of luminescent dyes efficiently quenched by O_2 are Pt(II)- and Pd(II)-porphyrins [37, 45, 46]. These molecular structures exhibit phosphorescence lifetimes in the range of 20–100 μs for Pt-porphyrins and 400–1,000 μs for Pd-porphyrins, which provide them from moderate to high quenchability by O_2. They have intense absorption bands in the near-UV (370–410 nm, Soret band) and visible (500–550 nm, Q-bands) regions, bright, well-resolved emission (630–700 nm) with relatively high quantum yields at physiological temperatures in aqueous solutions and solid-state formulations [37]. Some of the related structures, namely, the Pt- and Pd-complexes of benzoporphyrins, porphyrin-ketones and azaporphyrins, have longwave-shifted absorption (Q-bands > 600 nm) and phosphorescence in the very-near infrared region (700–900 nm). They are better suited for in vivo applications, but less compatible with standard photodetectors, such as PMT tubes. The structures of some dyes employed in O_2 sensors are shown in Fig. 1.1.

Phosphorescent O_2-sensitive materials are designed to attain the required physical, chemical, biological and O_2 quenching properties. For optimal analytical performance, sensor chemistry needs to be tailored to specific application, detection

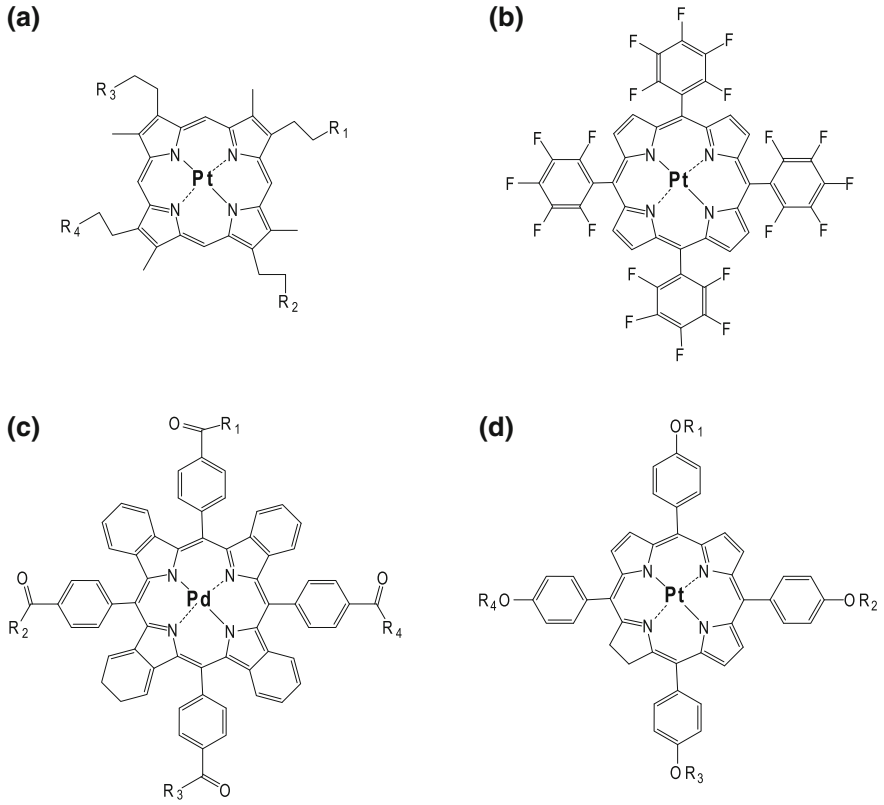

Fig. 1.1 Indicator dyes of porphyrin origin commonly used in O_2-sensitive materials. The derivatives of **a** Pt(II)-coproporphyrin–I (PtCP), R1 = R2 = R3 = R4 = COOH; **b** Pt(II)-meso-tetra-pentafluorophenyl porphyrin (PtPFPP); **c** meso-tetra(4-carboxyphenyl)tetrabenzoporphyrin (TPCTBP), R1 = R2 = R3 = R4 = OH; **d** meso-tetraarylporphyrin, R1 = R2 = R3 = R4—dendrimeric residues

platform and biological object being used. Thus, sensor excitation and emission spectra and photophysical properties (brightness, photostability) can be tuned by changing the macrocycle (e.g. CP, PFPP and TPCTBP). O_2 quenching efficiency and measurement range can be tuned by changing the central metal ion or microenvironment of the dye. Pt-porphyrins are less quenched and therefore better suited for the ambient O_2 range (0–200 μM), while Pd-porphyrins—for the low range 0–50 μM O_2. By introducing a dendrimeric shell or changing the polymeric matrix for dye encapsulation, one can alter the sensitivity to O_2 quenching [46–48]. Hydrophilicity can be improved by choosing the derivatives with polar side substituents on the macrocycle (e.g. CP, TPCTBP dendrimers), or by conjugating parent dye to a hydrophilic macromolecular carrier.

O_2 sensor material can be prepared as a macroscopic solid-state coating, microsensor deposited on the tip of optical fibre or liquid formulation—probe. Solid

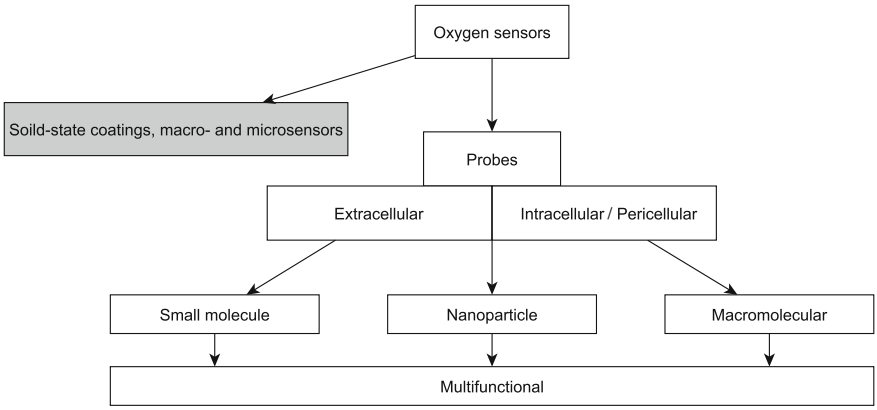

Fig. 1.2 Classification of O_2-sensing materials

state sensors have been used in coated microwell plates (BD Biosensor plate [49]), for the analysis of microbial and cellular respiration on a fluorescent reader (e.g. Mocon-Luxcel GreenLight® and Seahorse XF systems). O_2 microsensors [50] were applied to probe O_2 gradients in heterogeneous samples for single cell analysis [51], in microfluidic devices [52]. A number of solid-state O_2 sensors for O_2 measurement are produced commercially, for example, by Presens, Oxysense, Oxford Optronics, Mocon, Pyro Science, however, their main limitation is the lack of flexibility. Recent progress in this area is reviewed extensively [34, 52], so these systems are outside the scope of this book.

On the other hand, soluble O_2 probes provide greater flexibility and convenience for the users, and an extended range of applications [32]. The sensor can be added to the sample, dispensed, injected into tissue or animal and its working concentration is adjustable. Such a probe can be realised as a small molecule or supramolecular probes, nanoparticle and microparticle structures, which can also be combined with additional chemical, photophysical or biological functionality. Phosphorescent O_2-sensitive particles with magnetic properties have been described, which can be precipitated or localised within a sample with a magnet [48]. The main types of O_2 sensor materials are shown in Fig. 1.2.

1.4 Phosphorescent Probes for Sensing Cellular O_2

Within the group of *soluble O_2 probes* several categories can be defined. The small molecule probes are based on hydrophilic phosphorescent dyes or their derivatives bearing multiple polar or charged groups which provide them solubility in aqueous media. However, such probes have a tendency to bind non-specifically to proteins, cells and surfaces, display heterogeneity of their O_2 sensing properties and sensitivity to sample composition (pH, ionic strength, protein content).

These drawbacks can be partly addressed in the supramolecular probes in which several distinct functionalities are assembled together with the phosphorescent moiety in one chemical entity. Examples include the conjugates of PtCP dye with hydrophilic macromolecular carriers such as PEG or proteins (e.g. MitoXpress™ probe [53] used in cell based in vitro screening assays), and the more complex dendrimeric probes developed for O_2 imaging in tissue and vasculature [46]. In such dendrimeric probe (see Fig. 1.1), four peripheral carboxylic groups of the *meso*-substituted Pd/Pt-(benzo)porphyrin are modified with dendritic polyglutamic chains that shield the phosphor and reduce the influence of pH, ionic strength and medium components on the dye emission and quenching by O_2.

In order to achieve controlled and specific localisation of the sensor within the biological sample or bring additional functionality such as targeting the probe to extracellular, intravascular, intracellular or pericellular localisation, sensor material can undergo further chemical modification or coupling with a suitable delivery vector. Thus, to make the dendrimeric probe more soluble in aqueous media (plasma), prevent penetration inside the cells and keep it in the bloodstream, an additional hydrophilic shell was introduced by PEGylation [47]. To deliver O_2 probe inside the cell or to the cell surface, supramolecular structures are produced comprising the conjugates of phosphorescent dyes with cell-penetrating, intracellular targeting peptide sequences or receptor molecules (e.g. lectins or antibodies) [39, 54–57].

Nanoparticle-based probes undergo active development [58–62]. These structures typically have a size of 30–200 nm and consist of a polymeric matrix in which the indicator dye(s) is/are incorporated by chemical linkage to the polymer backbone or surface groups, or by physical inclusion in a gel, co-precipitation and formation of core–shell structures [61]. Various fabrication methods allow flexibility in the choice of indicator dyes, nanosensor matrix, size and surface modification. Thus, hydrophobic dyes, structures lacking functional groups (i.e. not suitable for the other probe types) and pairs of dyes (ratiometric or FRET-based O_2 sensing) can be introduced in such systems [62, 63]. A number of biocompatible polymers and co-polymers have been used, including polyacrylamide, silica, polystyrene, polyfluorene and hydrogels. Other advantages of the nanoparticle O_2 probes are the possibility to achieve high specific brightness and photostability, relative ease of fabrication and tuning of sensor properties. The challenges are: larger size compared to the molecular probes, variable size, distribution and physical properties, difficulties in controlling the composition and structure during fabrication, instability under prolonged storage (drying and sterilisation can be problematic), toxicity and lack of biocompatibility in in vivo applications for many of such probes.

Initially, cell-impermeable O_2 probes were applied to monitor bulk oxygenation and OCR of respiring samples. This approach has been productive, with a number of applications and screening systems developed and adopted by many users (see Chap. 2). Nowadays, there is a growing demand in probes that have different and better defined location within the biological sample, particularly in cells, tissue, organs and whole organism. There is also a growing demand in measurement

techniques and systems that allow probing and imaging of different O_2 pools in microscopic and macroscopic biological objects with high spatial resolution. With the advancement of probe and material chemistry and optical instrumentation, particularly fluorescence-based live cell imaging systems and sensitive time-resolved fluorescent readers, localised and targeted O_2 sensing approaches have become more common and available for ordinary users. Extensive experience of targeting small molecules to the cells and tissues (e.g. tumours) in drug delivery, MRI imaging and cancer therapy have been taken on board in O_2 sensing with a number of different types of probes with cell-penetrating capability, targeted to the membrane of mammalian cells and intracellular compartments described recently. These probes have opened the possibility to measure intracellular and pericellular O_2 concentrations and O_2 gradients between different compartments of respiring samples and within mammalian cells [55, 64].

The family of cell-targeted and intracellular probes have enabled in situ measurement of O_2 directly inside the cell, at cell surface and potentially in the mitochondria where most of O_2 gets consumed in mammalian cells and in peroxisomes for macrophages. In conjunction with high-resolution live cell imaging technique, this strategy provides the possibility to study intracellular O_2 gradient(s) with high selectivity, sensitivity and spatial resolution. This gives researchers a new level of detail about mitochondrial function, cell bioenergetics and biological roles of O_2. Rapid advancement of O_2-sensitive materials, new ways of intracellular delivery of small and large molecules and nanoparticle structures (e.g. by protein transduction domains, cell-penetrating peptide vectors) further extends our capabilities and allows new applications and O_2 sensing schemes.

The distinct photophysical characteristics of the phosphorescent O_2 probes provide large scope for multiplexing with other probes and parameters of cellular function, including Ca^{2+}, cellular ATP, NADH, mitochondrial and plasma membrane potentials, protein markers and fluorescent tags (GFP family). Several O_2 probes can be used with the same sample to monitor O_2 levels in different cellular compartments (intracellular, pericellular and extracellular O_2) and their dynamics upon changing cellular environment.

Some common phosphorescence-based O_2-sensitive probes designed for biological applications and their main photophysical and operational characteristics are described in Table 1.1.

1.5 Detection Modalities

Quenched-phosphorescence O_2 sensing can be realised by simple intensity-based, ratiometric or lifetime measurements. The main detection modalities are shown in Fig. 1.3.

Measurement of probe phosphorescence intensity is useful for qualitative and semi-quantitative assessment. The intensity signal is inversely related to O_2 concentration [see Eq. (1.2)]. However, in this mode, O_2 calibration is rather unstable

Table 1.1 An overview of O_2 sensing probes tested in biological applications (modified from [32])

Probe name and type	Application probe location	Equipment, detection mode	K_{s-v}, $\mu M^{-1}/\tau_0$, μs	Status, comments	References
Extracellular probes					
PdTPCPP (conjugated to BSA)—SM	O_2 mapping in tissues *Probe in blood/ vasculature*	Ex—416, 523 nm Em—690 nm Scanning phosphorescence quenching microscopy	0.382/ ~700	Quantitative Point measurement Used by several labs	[31, 65–70]
Oxyphor R2 (PdTPCPP dendrimer)—SM	O_2 mapping in tissues *Probe in blood/ vasculature*	Phase fluorometry: Ex—524 nm Em—690 nm 4 mm light guide; Two-photon microscope	0.343/640 (38 °C, pH 7.4)	Quantitative Point measurement Used by several labs	[46, 71]
Oxyphor G2 (PdTCPTBP dendrimer)—SM	Tissue O_2 gradients in vivo *Probe in blood/ vasculature*	Wide field FLIM: Ex—440/632 nm, Em—790 nm	0.086/251 (38 °C, pH 7.4)	Quantitative Used by several labs and with different models	[46, 72]
MitoXpress (PtCP conjugate)—SM	OCR by cells, mitochondria, enzymes. Assessment of cell bioenergetics *Probe added to the medium*	TR-F reader, RLD: Ex—340–420 nm Em—640–660 nm	0.04/67	Quantitative. Used by many labs. Validated in drug and toxicity screening	[53, 55, 73–75]
PtP-C343 (PtTAOP-Coumarin 343 dendrimer)—SM	Tissue O_2. In vivo O_2 gradients *Probe in blood/ vasculature*	Two-photon FLIM: Ex—840 nm Em—682 nm	>0.11/60	Quantitative. Require special equipment and setup Used in several labs	[47, 76, 77].

(continued)

Table 1.1 (continued)

Probe name andtype	Applicationprobe location	Equipment, detection mode	K_{s-v}, $\mu M^{-1}/\tau_0$, μs	Status, comments	References
Oxyphors R4 and G4	Tissue O_2 gradients in vivo. Tumour imaging *EC probe in blood/ vasculature/ interstitial space*	Wide-field FLIM Ex—428, 530 nm (R4); 448, 637 (G4) Em—698 (R4), 813 (G4)	R4: 0.098/681 (37 °C, pH 7.2) G4: 0.083/218 (38.2 °C, pH 7.2)	Quantitative. Require special equipment and setup	[78]
PS-NP (polystyrene NP doped with PdTPTBP and DY635—reference)	Targeted tumour in vivo imaging *EC probe*	Ratiometric-based Lifetime-based Ex—635 nm Em—670 nm (reference); 800 nm (O_2 sensitive)	ND	Quantitative. May be used for intracellular measurement with modified coating	[79]
Pericellular probes					
ER9Q-PtCP (PtCP protein conjugate)—SM	Cell oxygenation assessment of intracellular O_2 gradient *Stains plasma membrane of cultured cells*	TR-F reader, RLD: Ex—340–420 nm Em—640–660 nm	0.046/55	Quantitative 2 cell lines tested (PC12, MEF)	[55]
Intracellular probes					
MitoXpress (PtCP conjugate)—SM	Cell oxygenation Metabolic responses *Impermeable probe delivered into the cell with Endo-Porter*	TR-F reader, RLD: Ex—340–420 nm Em—640–660 nm	~0.04/67	Quantitative Facilitated loading required (24–28 h); 6 cell types tested (cell-specific)	[64, 80–83]

(continued)

Table 1.1 (continued)

Probe name andtype	Applicationprobe location	Equipment, detection mode	K_{s-v}, $\mu M^{-1}/\tau_0$, μs	Status, comments	References
O_2 PEBBLEs (PtOEPK & OEP, ormosil)—NP	Cell oxygenation *Impermeable probe delivered into the cell with gene gun*	Ratiometric wide field imaging Ex—568 nm, Em—620/750 nm	0.032/ND	Semi-quantitative (relative) Stressful loading 1 cell type tested	[84]
Ru(II)-(py)$_3$-R$_8$ (peptide conjugate)—SM	O2 mapping in cells *Cell-permeable, self-loading probe*	Wide field FLIM: Ex—460 nm Em—607 nm	ND	Semi-quantitative 1 cell type tested	[39]
Cell penetrating PtCP peptide conjugates: PtCPTE-CFR$_9$, PEPP0-5, T1-T4—SM	Cell oxygenation, Metabolic responses *Cell-permeable, self-loading probe*	TR-F reader, RLD: Ex—340–420 nm Em—640–660 nm Intravital confocal imaging was also demonstrated	~0.006/70	Quantitative >6 cell lines tested Controlled sub-cellular location	[54, 56, 85, 86]
PtOEP/PDHF and PFO—NP	O_2 mapping in cells *Probe uptake by macrophages*	Ratiometric wide field imaging: Ex—350 nm Em—440/650 nm	ND	Semi-quantitative One cell line tested (macrophages) particle variability, require UV excitation	[62]
Near infrared PAA NPs (Oxyphor G2 probe in PAA gel, with peptide coat)—NP	Cell oxygenation *Cell permeable, self-loading probe*	Wide field and confocal imaging: Ex—633 nm Em—790 nm	0.034/ND (37 °C) (without cells)	Quantitative Several cell lines tested. High probe concentrations used Cross-sensitivity to pH	[59]

(continued)

Table 1.1 (continued)

Probe name andtype	Applicationprobe location	Equipment, detection mode	K_{s-v}, $\mu M^{-1}/\tau_0$, μs	Status, comments	References
RGB NPs (PtPFPP & BCPN in aminated polystyrene)—NP	Cell oxygenation *Cell permeable, self-loading probe*	Wide-field RGB imaging: Ex—330–380 nm Em—Red, Green	~0.0083/NA	Semi-quantitative 1 cell line tested. NP variability, long loading—48 h	[63]
MitoXpress-Intra (NANO2, PtPFPP in RL100 polymer)—NP	Cell oxygenation. Metabolic responses, cell bioenergetics *Cell permeable, self-loading probe*	TR-F reader: RLD Ex—340–420 nm Em—640–660 nm wide-field FLIM and confocal O_2 imaging	0.04/69	Quantitative >5 cell lines tested High brightness and photostability	[55, 87]
Cell penetrating IrOEP peptide conjugates: Ir1, Ir2,—SM	Cell oxygenation, Metabolic responses *Cell-permeable, self-loading probe*	TR-F reader, RLD: Ex—390 nm Em—650 nm	Ir1: 0.074(Ksv1)/58 Ir2: ND/69	Quantitative >5 cell lines tested	[57]
MM2 (PtPFPP, PFO in RL100 polymer)—NP	Cell oxygenation Metabolic responses, cell bioenergetics *Cell permeable, self-loading probe*	TR-F reader: RLD, FLIM, ratiometric intensity, multiphoton microscopy Ex—400 nm (single photon), 760 nm (two photon) Em—430, 650	0.04/61	Quantitative Tested with 2D and 3D cell samples	[88]

Note K_{s-v} constants were calculated based on the published data. At normal atmospheric pressure O_2 has 160 mmHg with dissolved concentration ~200 μM or 4,950 ppm

PAA polyacrylamide hydrogel; *PDHF* poly(9,9-dihexylfluorene)); *PFO* (poly(9,9-diheptylfluorene-alt-9,9-di-p-tolyl-9H-fluorene)); *SM* supramolecular; *NA* not applicable; *ND* no data reported; *NP* nanoparticle-based; *BCPN* butyl-N-(5-carboxypentyl)-4-piperidino-1,8-naphthalimide

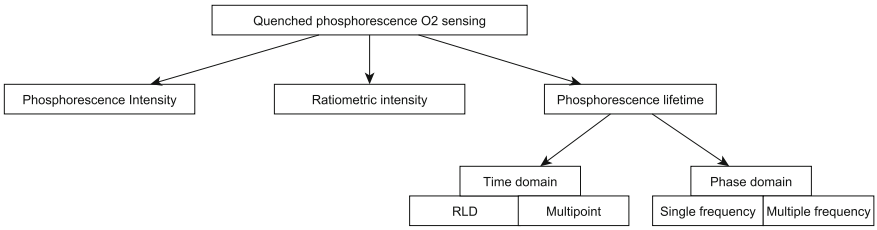

Fig. 1.3 Measurement modalities in O_2 sensing

and influenced by probe concentration, its photodegradation, measurement geometry, optical properties of the sample, drift and noise of the detector and light source. On the other hand, under standard conditions, relative changes in O_2 and OCR (e.g. treated versus untreated cells) can be measured easily and reliably in this mode.

Introduction of a reference (O_2-insensitive) dye in the sensor allows parallel intensity measurements in two spectral channels and determination of O_2 concentration from the ratio of the O_2 sensitive and O_2-insensitive signals. This approach overcomes many of the limitations of single channel measurements and makes O_2 calibration more stable and suitable for quantitative O_2 sensing. In certain cases, linear relationship of the ratio signal and O_2 concentration can be achieved. Nonetheless, the signal ratio can be influenced by the sample and detection system, especially when the two specific signals are of moderate or low intensity (low signal to noise/blank ratio). Factors such as instability of the detector and excitation source, differential scattering, autofluorescence and detector dark counts in the two spectral regions, different photobleaching rates of the two dyes can contribute and cause a drift or shift in O_2 calibration. Due to the relatively simple optical set-up, well-established instrumentation and measurement procedures for fluorescence ratiometric and intensity-based O_2 sensing can be implemented on a wide range of detection platforms available in ordinary research labs. However, one should use them with care to avoid measurement artefacts and experimental errors in O_2 quantification.

Phosphorescence lifetime-based O_2 sensing is by far regarded as the most stable and accurate modality for O_2 sensing [33]. Although instrumentation for luminescence lifetime measurements is somewhat more complex and less common than intensity-based systems, it is rapidly gaining popularity in life sciences since it can overcome many of the limitations of fluorescence intensity-based systems and provide higher confidence and stability in O_2 measurement. Measurement of phosphorescence lifetimes, which lay in the microsecond time domain, is technically simple, but often requires dedicated hardware, signal acquisition and processing algorithms to implement reliable and on-the-fly determination of probe lifetime. One such method is phase-fluorometry, in which the sample is excited with periodically modulated light (sine of square wave excitation at kHz frequencies) and detector optoelectronics measures the phase shift of luminescent

signal with respect to excitation, ϕ. From the measured ϕ (degrees angle) phosphorescence lifetime of the probe is calculated as:

$$\tau = \mathrm{tg}(\phi)/2\pi v \tag{1.3}$$

where v is modulation frequency of excitation (Hz), and O_2 concentration is calculated according to Eq. (1.2) [89].

An alternative method is based on direct measurement of the phosphorescence decay under short-pulse excitation (<10 μs), using a multi-channel scaler with photon counting detector or Time-Correlated Single Photon Counting (TCSPC) board [42]. A simplified version of this method is called Rapid Lifetime Determination (RLD), in which emission intensity signals (F_1, F_2) are collected at two different delay times (t_1, t_2) after the excitation pulse and lifetime is calculated as follows [82]:

$$\tau = (t_2 - t_1)/\ln(F_1/F_2) \tag{1.4}$$

Time-resolved detection in the microsecond range also allows effective elimination of sample autofluorescence and scattering, providing large improvement in sensitivity and selectivity of probe detection and reduced interferences. As a result, RLD usually provides good accuracy and resolution in the measurement of phosphorescence lifetimes of O_2 sensitive materials (including the intracellular O_2 probes) and quantification of O_2 concentration in complex biological samples. It should be noted though that RLD operates reliably only when blank signals are low and specific signals high, i.e. S:N > 5 [82]. Modern instruments often have built-in microsecond time-resolved fluorometry (TR-F) and lifetime measurement capabilities, which make them suitable for O_2 sensing with the phosphorescent porphyrin probes. Examples include the multi-label fluorescence readers for assays in microplates, screening systems, wide-field or laser-scanning microscopes that support time-domain and phase-domain FLIM mode. At the same time, such instruments need to be assessed thoroughly to ensure their performance with the probe, including the sensitivity, reproducibility and accuracy of lifetime measurements, as well as temperature control and uniformity of readings across the plate. Many commercial systems cannot provide adequate performance in the measurement of short lifetimes of Pt-porphyrins and/or longwave emission of meso-substituted and benzo-porphyrins.

The core detection modalities described above can be realised as 'cuvette' format, in which the optical signal and O_2 concentration are measured at one point or for the whole sample (macroscopic) on a suitable luminescent spectrometer or reader. Using epifluorescence alignment of the optics and an X–Y stage, measurement of multiple points/samples or two-dimensional (2-D) scanning with sub-mm resolution can be implemented in multi-well plates or other substrates. If an O_2 probe is introduced in a particular compartment (e.g. intracellular or pericellular), one can achieve measurement of *local* concentrations and gradients of O_2 within the sample. Alternatively, quenched-phosphorescence detection can be coupled with an imaging detector, thus enabling O_2 imaging within the sample, for example, on a fluorescence

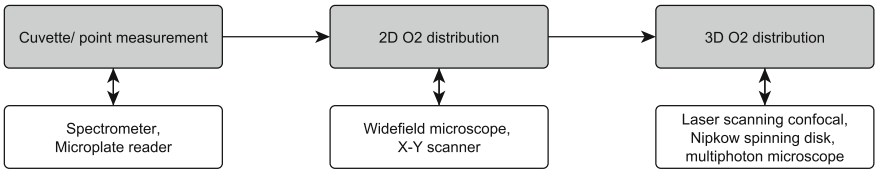

Fig. 1.4 O_2 measurement tasks and detection platforms for various experimental needs

microscope, live cell imaging (LCI) or macroscopic imaging systems. The main measurement tasks and detection options are shown schematically in Fig. 1.4).

Relatively simple and inexpensive wide-field fluorescence microscopes operating in intensity and ratiometric mode can provide 2-D visualisation of respiring objects stained with an O_2 probe, with sub-cellular spatial resolution. Relative oxygenation and changes related to sample respiration activity can be monitored performing time-lapse imaging experiments. Furthermore, confocal microscopy represented by laser-scanning and spinning disk fluorescence LCI systems enables the analysis of 3-D O_2 distribution in complex objects with sub-micron spatial resolution. Compared to the traditional microscopes exciting the luminophores in one-photon mode, the multi-photon imaging systems employ high-power femtosecond NIR lasers for excitation which provide better contrast and spatial resolution and deep penetration into tissue (>500 μm). However, such systems are more expensive and they require special indicator dyes with large cross-section of two-photon absorption, and to be able to see the long-decay emission of the probes and their response to O_2, system hardware and software need to be specially tuned [90, 91]. A number of dedicated O_2 probes with two-photon and FRET antennae, imaging systems and applications on their basis have been described recently, and this area continues to develop rapidly [47, 62, 78, 92].

Fluorescence/Phosphorescence Lifetime Imaging Microscopy (FLIM/PLIM, also called PQM—Phosphorescence Quenching Microscopy [93]) enables more reliable visualisation of O_2 distribution in complex biological samples, and accurate quantification of O_2. Wide-field microscopes equipped with gated CCD camera and LED/laser excitation providing trains of ns-μs pulses at kHz frequency can generate 2-D O_2 images with single cell resolution [66, 67, 76, 94]. Following each excitation pulse and a time delay (variable), emitted photons are collected by the camera over the measurement window time and integrated over a number of pulses to generate an intensity frame. This is repeated at several delay times, and from this set of frames emission decay is reconstructed and lifetime is determined for each pixel of the CCD matrix. By applying probe calibration function (determined in a separate experiment), lifetime images of the sample can be converted into O_2 concentration map.

For the laser-scanning systems, emission lifetimes are measured sequentially for each pixel with a PMT or photodiode detector, processed by the software to generate 2-D images of Z-stacks which are then assembled together to produce 3-D O_2 maps. Several custom-built PLIM systems employing detection and lifetime determination with TCSPC under both one-photon and two-photon excitation have

been described in recent years and applied to O_2 imaging of live tissue in animal models. A dedicated hybrid ns/ms FLIM/PLIM hardware optimised for phosphorescence lifetime imaging and O_2 sensing experiments is produced commercially, by Becker & Hickl GmbH for example [42, 95].

In high-resolution microscopic imaging of O_2, samples are exposed to high illumination intensities and probe photostability becomes a critical issue. Many O_2–sensitive dyes and probes on their basis lack photostability. Perfluorinated PtPFPP dye is regarded as one of the most photostable dyes for such applications [87]. O_2 imaging experiments require thorough optimisation to produce sufficiently high, reliably measurable luminescent signals along with low phototoxicity, cell damage and photobleaching. In addition, careful calibration (measuring probe signal at several known pO_2 levels) is required to be able to convert raw fluorescence intensity images into O_2 concentration maps.

1.6 Measurement Formats Used in Optical O_2 Sensing

The various probe chemistries, detection modalities and platforms enable realisation of O_2 sensing in different measurement formats, thus making it versatile and suitable for a broad range of analytical tasks and applications. Some of these formats allow high sample throughput, high information content and multiplexing with the other biomarkers and parameters of cellular function.

The traditional set-up for O_2 respirometry is an air-tight cell, such as quartz cuvette with a stopper, which accommodates the biological sample along with the probe and is measured on a spectrometer to determine probe phosphorescent signal and changes over time and relate them to O_2 concentration or OCR, respectively. For accurate quantification, the anaerobic cuvette should contain no headspace or bubbles (air has much higher capacity for O_2 than aqueous media, and this may skew the results), be sealed, maintained at constant temperature (37 °C is optimal for eukaryotic cells), and stirred to distribute the respiring matter uniformly. At the same time, there is a growing need to conduct rapid, parallel O_2 sensing experiments with large number of biological samples (different cells, drugs, conditions, replicates and controls), to use the existing detection and screening platforms and miniaturise the bioassays. Sets of several anaerobic micro-cuvettes can be aligned on a multi-cell holder of a fluorescent reader, but this still does not provide the required sample throughput and requires modifications to the conventional anaerobic cuvette format. Examples of specialised substrates for optical O_2 sensing and respirometry include narrow-bore capillary cuvettes from the LightCycler® system measured on a carousel by dedicated detector (originally developed for quantitative PCR), standard microtiter plates with and without oil seal, low-volume sealable microplates, microfluidic biochips and perfusion chambers [36, 73, 75, 96, 97]. The common measurement formats are shown schematically in Fig. 1.5.

In particular, conventional microtiter plates provide large time savings, and reduced use of valuable and perishable biomaterials with drifting activity. They

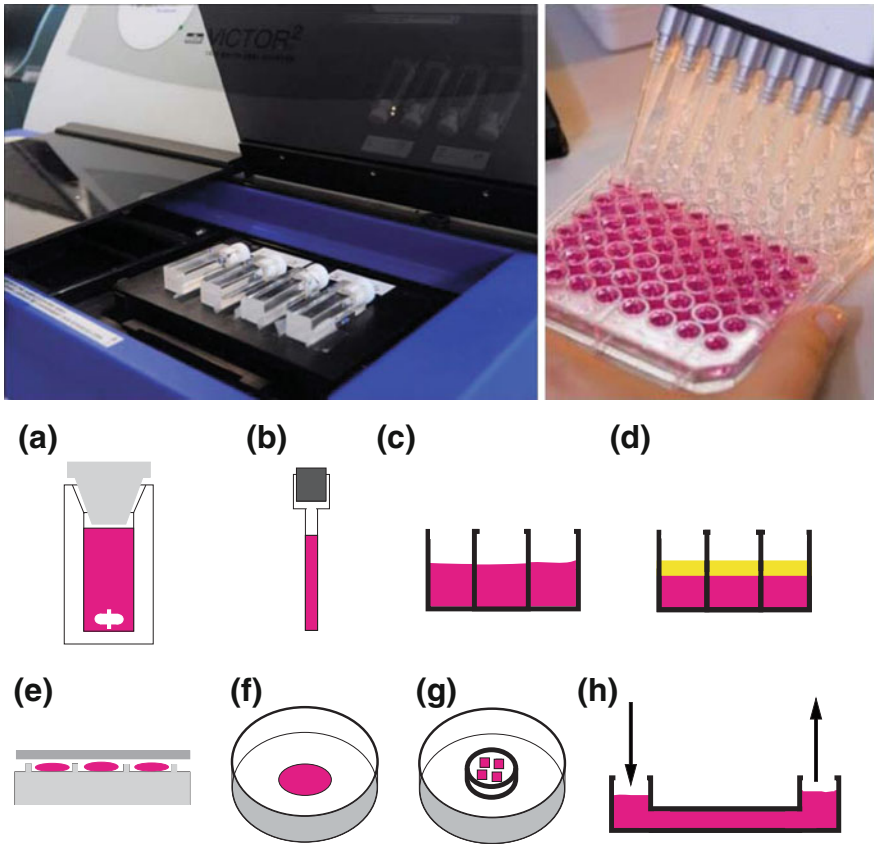

Fig. 1.5 Different measurement set-ups and substrates employed in optical O_2 sensing. *Top panel* Anaerobic micro-cuvettes (*left*) and 96-well plate with mammalian cells (*right*) being prepared for respirometric measurements on a commercial TR-F reader. *Bottom panel*. **a** sealed quartz cuvette with stirrer; **b** glass capillary cuvette (operate on the LightCycler® quantitative PCR instrument **c**, **d** microplate with sample wells unsealed (**c**) or sealed with the layer of oil (**d**); **e** Sealable low-volume microplate (Luxcel); **f**, **g** glass-bottom minidish for biological samples adapted for analysis of single (**f**) or multiple (**g**) samples (Ibidi); **h** Microfluidic biochips and perfusion flow chambers. The biomaterial analysed is shown in *pink colour*

facilitate assay miniaturisation (96- and 384-well plates are the most common), the use of automated liquid handling equipment (multichannel pipettes, dispensers and robots) and multi-label fluorescent or TR-F readers available in many labs. On the other hand, respirometric assays in microplates often have compromised performance. Thus, due to partial sealing of samples (oil seal and plastic body of the plate still allow ambient O_2 to diffuse in), assay sensitivity is reduced and usually *relative* but not absolute OCRs can be assessed reliably. Slow temperature equilibration requires care when preparing the plate, analysing signal profiles (negative slopes at the start of the assay are common) and getting consistent results in all wells across the plate.

Another measurement format represents a vessel with medium and respiring material exposed to a gaseous atmosphere such as ambient air. This format can be used to detect microbial growth/respiration in microplates with built-in O_2 sensors (BD Biosciences). Generally, such assays require relatively high levels of respiration and are more easily affected by sample distortion (respiration profiles are less reproducible compared e.g. to oil-sealed samples). With the development of intracellular (cell-permeable) O_2 probes, the range of analytical tasks that can be conducted in this manner have been extended. In particular monitoring of in situ oxygenation, respiratory activity and responses to metabolic stimulation of adherent cell cultures [56, 64, 82], analysis and imaging of O_2 in complex objects such as heterogeneous populations of cells, tissue slices, spheroids, small organisms, experiments under hypoxia in which the operator can precisely control atmospheric pO_2 and/or cellular O_2 levels, and conduct mechanistic biological studies under such conditions can be conducted using this simple format. It is also quite common in imaging experiments where glass-bottom minidishes with cells are commonly used. The latter can also be used with silicon microchamber inserts dividing the sample into several compartments (Fig. 1.5).

1.7 Biological Applications of Optical O_2 Sensing

The existing range of different probes, measurement formats and detection modalities for O_2 sensing open a large scope for the use of these techniques in various biological and physiological studies. One of the main advantages of the optical O_2 sensing technique is the possibility of contactless and minimally invasive measurements with gentle biological samples. The probe can be simply introduced into the sample and then interrogated with an external detector which measures probe luminescent signal and converts it into O_2 concentration.

These applications can be grouped into several categories:

- *Analysis of homogeneous, macroscopic samples* for example, monitoring of enzymatic O_2 consumption, quantification of activity and inhibition of important enzymes (e.g. cyclooxygenase, monoamino oxidase or cytochrome p450 oxidase [97]), determination of their substrates and metabolites present in test sample, enzyme biosensors (e.g. for glucose, lactate). Similarly, OCR and activity of mitochondrial preparations (e.g. from rat liver, heart, brain, human tissue) can be analysed under different conditions (e.g. State 2 and State 3 respiration, inhibition and uncoupling with drugs [3]), so metabolic activity and proliferation rate of suspension eukaryotic cells can be assessed (yeast, mammalian cells [36, 53, 98]). Quickly proliferating microbial cells which produce characteristic respiration profiles with a steep transition from aerated to deoxygenated condition, have to be analysed differently [99]. All these respirometric assays and applications can be conducted in a simple mix-and-measure procedure in standard 96-or 384-well plates on a standard plate reader.

- *Physiological studies with cultures of adherent mammalian cells (monolayers, 2-D models)* is inarguably the largest and most important group of in vitro assays. They are now widely used in various areas of life sciences and biomedical research, including general cell biology, disease models, drug development, biochemical toxicology, drug safety assessment, environmental monitoring. It includes the analysis of cell respiration, assessment of cell bioenergetics and metabolic status (in conjunction with the other biomarkers), comparison of normal and transformed cells, monitoring changes in cellular function and relating them to disease state or therapeutic treatment. Such assays are easy to perform in microtiter plates with extracellular O_2 probes such as MitoXpress [35, 75, 81, 100–102]. OCR measurements can be multiplexed with other probes (extracellular acidification, cellular ATP, Ca^{2+}, ROS, MMP) to achieve high-throughput multi-parametric assessment.
- *Control of cell oxygenation and experiments under hypoxia*. Live cells constantly consume O_2, which provides them energy in the form of ATP and also acts as a substrate in numerous biochemical reactions, thus acting as O_2 sink [7, 103]. Despite the efficient supply by the blood vessels and vasculature and rapid diffusion of O_2 across the cells and tissue, cells and tissues deoxygenate their environment and function under reduced O_2 levels (compared to ambient 21 % of O_2). On the other hand, most of the cell culture work is still performed at ambient O_2 (21 % in the atmosphere) which is regarded as a hyperoxia at which the cells experience oxidative stress and may behave differently to the in vivo conditions. This is particularly important for research in area of cancer and stem cells which normally reside in hypoxic or anoxic niches [104]. Intracellular O_2 probes provide useful tools for in situ control of oxygenation of cell monolayers and individual cells under ambient and hypoxic conditions, and to study adaptive responses of cells to hypoxia, drug action, signalling and cells physiology, particularly for neuronal cells [80, 105].
- In vitro *analysis of heterogeneous 2D and 3D respiring objects* including mixed cultures of different cells (co-cultures), 3-D scaffolds and spheroids (e.g. neurospheres), samples of animal tissue (slices) cultured under static or perfused conditions. Such systems represent the native microenvironment of mammalian cells in vivo more closely, and therefore represent more relevant cell models.
- In vivo *imaging* of tissue O_2 is of high fundamental and practical importance. Measurement of actual oxygenation in live respiring tissue (e.g. brain or muscle), localised O_2 gradients in the vasculature (blood vessels, capillaries) or tumour oxygenation can be realised using extracellular O_2 probes and phosphorescence lifetime-based O_2 imaging [65, 66, 68, 71, 72, 106–108]. This was also realised in plant cells [50]. In the last few years, wide-field FLIM systems and high-resolution confocal and two-photon laser-scanning systems [109] for imaging tissue O_2 were successfully used in complex in vivo and ex vivo studies. Thus, the dendrimeric probe PtP-C343 was injected in the blood stream and used to measure local oxygenation in rodent brain at different distances from arterial regions on a two-photon FLIM LCI system [76]. Such studies normally require special setup, measurement equipment, skills and ethical

approval for animal work. Due to our limited experience, we are not describing them in great detail.

- Ex vivo *imaging of O_2 in perfused organs and tissues*. This is performed similarly to the above in vivo sensing of O_2. Thus, mapping of O_2 in rodent retina [69, 72], dynamics of O_2 in individual frog skeletal muscle fibres [110]; imaging of oxygenation of tumours [79, 111] and O_2 in microcirculation [65, 66] were reported. Oxygenation of carotid body explant was monitored with the intracellular O_2 probe and correlated to cellular Ca^{2+} levels [85].
- *Assessment of intracellular O_2 gradients.* This area still remains obscure. Robiolio et al. reported O_2 gradients in neuroblastoma cells [112], but then other groups failed to detect such gradients in vascular [77] and hepatic Hep3B cells [30]. Parallel measurement of mitochondrial O_2 with endogenous protoporphyrin IX delayed fluorescence and extracellular O_2 with Oxyphor G2 probe revealed marginally small gradients: $\sim$2 Torr in resting and $\sim$4 Torr in uncoupled neuroblastoma and fibroblast cells [26]. For intact rat liver even at low ambient O_2, mito O_2 still had high values [25]. Significant intra-tissue heterogeneity and possible icO_2 gradient were reported for heart tissue [113]. Introduction of new O_2 probes targeted to intracellular compartments and cell membrane will help to advance this field [55], and clarify possible inconsistencies and experimental artefacts from the above studies.
- *Other groups including O_2 measurement in photosynthetic systems, small organisms and microfluidic biochips.* Plants produce O_2 by photosynthesis during light phase, and consume O_2 during dark phase [34, 50, 114]. Aquatic and underground organisms (i.e. round worms *C.elegans, zebrafish Danio rerio, Daphnia*) also experience hypoxia in their habitat [115]. Studies of behaviour of these model animals under hypoxic conditions and in various physiological and toxicological studies are on the rise. In situ control of oxygenation in cultures of these organisms, within individual animals and their microenvironment is important from the biological and physiological points of view. Other attractive models include artificially engineered mammalian tissues and organs, microfluidic devices, cell and tissue-based biochips [116].

A number of representative examples covering the above applications with different biological models and studies are described in greater detail in the following two experimental Chapters. Chapter 2 is focused on plate reader analysis of macroscopic samples, including eukaryotic and prokaryotic cells, spheroids, enzymes, small organisms, comparison of different cells, drugs and treatments. Chapter 3 describes on O_2 imaging in individual cells, complex 3D objects with high level of detalisation and generation of 2-D and 3-D O_2 maps and time profiles of oxygenation.

Acknowledgments This work was supported by the Science Foundation Ireland, grant 07/IN.1/B1804 and the Ministry of Education and Science of Russian Federation, State Contract No 14.740.11.0909.

References

1. Semenza GL (2007) Life with oxygen. Science 318(5847):62–64
2. Devor A, Sakadzic S, Srinivasan VJ, Yaseen MA, Nizar K, Saisan PA, Tian P, Dale AM, Vinogradov SA, Franceschini MA, Boas DA (2012) Frontiers in optical imaging of cerebral blood flow and metabolism. J Cereb Blood Flow Metab 32(7):1259–1276. doi:10.1038/jcbfm.2011.195
3. Brand MD, Nicholls DG (2011) Assessing mitochondrial dysfunction in cells. Biochem J 435(2):297–312. doi:10.1042/bj20110162
4. Wilson DF, Finikova OS, Lebedev AY, Apreleva S, Pastuszko A, Lee WMF, Vinogradov SA (2011) Measuring oxygen in living tissue: intravascular, interstitial, and "tissue" oxygen measurements. In: LaManna JC, Puchowicz MA, Xu K, Harrison DK, Bruley DF (eds) Advances in experimental medicine and biology, vol 701. Springer, US, pp 53–59. doi:10.1007/978-1-4419-7756-4_8
5. Semenza GL (2007) Oxygen-dependent regulation of mitochondrial respiration by hypoxia-inducible factor 1. Biochem J 405(1):1–9
6. Wilson DF (2008) Quantifying the role of oxygen pressure in tissue function. Am J Physiol Heart Circ Physiol 294(1):H11–H13. doi:01293.200710.1152/ajpheart.01293.2007
7. Erecinska M, Silver IA (2001) Tissue oxygen tension and brain sensitivity to hypoxia. Respir Physiol 128(3):263–276
8. Jezek P, Plecitá-Hlavatá L, Smolková K, Rossignol R (2010) Distinctions and similarities of cell bioenergetics and the role of mitochondria in hypoxia, cancer, and embryonic development. Int J Biochem Cell biol 42(5):604–622
9. Lin J, Handschin C, Spiegelman BM (2005) Metabolic control through the PGC-1 family of transcription coactivators. Cell Metab 1(6):361–370
10. Bartrons R, Caro J (2007) Hypoxia, glucose metabolism and the Warburg's effect. J Bioenerg Biomembr 39(3):223–229
11. De Filippis L, Delia D (2011) Hypoxia in the regulation of neural stem cells. Cell Mol Life Sci 68(17):2831–2844. doi:10.1007/s00018-011-0723-5
12. Takahashi E, Doi K (1998) Impact of diffusional oxygen transport on oxidative metabolism in the heart. Jpn J Physiol 48(4):243–252
13. Palm F, Nordquist L (2011) Renal oxidative stress, oxygenation, and hypertension. Am J Physiol Regul Integr Comp Physiol 301(5):R1229–R1241. doi:10.1152/ajpregu.00720.2010
14. Wagner PD (2012) Muscle intracellular oxygenation during exercise: optimization for oxygen transport, metabolism, and adaptive change. Eur J appl Physiol 112(1):1–8. doi:10.1007/s00421-011-1955-7
15. Clark LC, Wolf R, Granger D, Taylor Z (1953) Continuous recording of blood oxygen tensions by polarography. J Appl Physiol 6(3):189–193
16. Wu C–C, Luk H-N, Lin Y-TT, Yuan C-Y (2010) A Clark-type oxygen chip for in situ estimation of the respiratory activity of adhering cells. Talanta 81(1–2):228–234
17. Jekabsons MB, Nicholls DG (2004) In situ respiration and bioenergetic status of mitochondria in primary cerebellar granule neuronal cultures exposed continuously to glutamate. J Biol Chem 279(31):32989–33000. doi:10.1074/jbc.M401540200
18. Yadava N, Nicholls DG (2007) Spare respiratory capacity rather than oxidative stress regulates glutamate excitotoxicity after partial respiratory inhibition of mitochondrial complex I with rotenone. J Neurosci 27(27):7310–7317. doi:10.1523/jneurosci.0212-07.2007
19. Williams BB, Khan N, Zaki B, Hartford A, Ernstoff MS, Swartz HM (2010) Clinical electron paramagnetic resonance (EPR) oximetry using India ink. In: Takahashi E, Bruley DF (eds) Advances in experimental medicine and biology, vol 662. Springer US, pp 149–156. doi:10.1007/978-1-4419-1241-1_21
20. Liu Y, Villamena FA, Sun J, Wang TY, Zweier JL (2009) Esterified trityl radicals as intracellular oxygen probes. Free Radic Biol Med 46(7):876–883

21. Bobko AA, Dhimitruka I, Eubank TD, Marsh CB, Zweier JL, Khramtsov VV (2009) Trityl-based EPR probe with enhanced sensitivity to oxygen. Free Radic Biol Med 47(5):654–658
22. Halevy R, Shtirberg L, Shklyar M, Blank A (2010) Electron spin resonance micro-imaging of live species for oxygen mapping. J Vis Exp 42:e2122
23. Wittenberg JB (1970) Myoglobin-facilitated oxygen diffusion: role of myoglobin in oxygen entry into muscle. Physiol Rev 50(4):559–636
24. Foster KA, Galeffi F, Gerich FJ, Turner DA, Müller M (2006) Optical and pharmacological tools to investigate the role of mitochondria during oxidative stress and neurodegeneration. Prog Neurobiol 79(3):136–171
25. Mik EG, Johannes T, Zuurbier CJ, Heinen A, Houben-Weerts JHPM, Balestra GM, Stap J, Beek JF, Ince C (2008) In vivo mitochondrial oxygen tension measured by a delayed fluorescence lifetime technique. Biophys J 95(8):3977–3990
26. Mik EG, Stap J, Sinaasappel M, Beek JF, Aten JA, van Leeuwen TG, Ince C (2006) Mitochondrial PO2 measured by delayed fluorescence of endogenous protoporphyrin IX. Nat Meth 3(11):939–945
27. Ashkenazi S, Huang S-W, Horvath T, Koo Y-EL, Kopelman R (2008) Photoacoustic probing of fluorophore excited state lifetime with application to oxygen sensing. J Biomed Opt 13(3):034023–034024
28. Potzkei J, Kunze M, Drepper T, Gensch T, Jaeger K-E, Buechs J (2012) Real-time determination of intracellular oxygen in bacteria using a genetically encoded FRET-based biosensor. BMC Biol 10(1):28
29. Takahashi E, Sato M (2010) Intracellular diffusion of oxygen and hypoxic sensing: role of mitochondrial respiration new frontiers in respiratory control. In: Homma I, Fukuchi Y, Onimaru H (eds) Advances in experimental medicine and biology, vol 669. Springer, New York, pp 213–217. doi:10.1007/978-1-4419-5692-7_43
30. Takahashi E, Takano T, Nomura Y, Okano S, Nakajima O, Sato M (2006) In vivo oxygen imaging using green fluorescent protein. Am J Physiol Cell Physiol 291(4):C781–C787. doi:10.1152/ajpcell.00067.2006
31. Vanderkooi JM, Maniara G, Green TJ, Wilson DF (1987) An optical method for measurement of dioxygen concentration based upon quenching of phosphorescence. J Biol Chem 262(12):5476–5482
32. Dmitriev RI, Papkovsky DB (2012) Optical probes and techniques for O(2) measurement in live cells and tissue. Cell Mol Life Sci CMLS. doi:10.1007/s00018-011-0914-0
33. Papkovsky DB (2004) Methods in optical oxygen sensing: protocols and critical analyses. Methods Enzymol 381:715–735. doi:10.1016/S0076-6879(04)81046-2S0076687904810462
34. Ast C, Schmälzlin E, Löhmannsröben H-G, van Dongen JT (2012) Optical oxygen micro- and nanosensors for plant applications. Sensors 12(6):7015–7032
35. Gerencser AA, Neilson A, Choi SW, Edman U, Yadava N, Oh RJ, Ferrick DA, Nicholls DG, Brand MD (2009) Quantitative microplate-based respirometry with correction for oxygen diffusion. Anal Chem 81(16):6868–6878. doi:10.1021/ac900881z
36. Hynes J, Natoli E, Jr., Will Y (2009) Fluorescent pH and oxygen probes of the assessment of mitochondrial toxicity in isolated mitochondria and whole cells. Curr Protoc Toxicol Chapter 2 Unit 2 16. doi:10.1002/0471140856.tx0216s40
37. Papkovsky DB, O'Riordan TC (2005) Emerging applications of phosphorescent metalloporphyrins. J Fluoresc 15(4):569–584. doi:10.1007/s10895-005-2830-x
38. Yoshihara T, Yamaguchi Y, Hosaka M, Takeuchi T, Tobita S (2012) Ratiometric molecular sensor for monitoring oxygen levels in living cells. Angew Chemie Int Ed 51(17):4148–4151. doi:10.1002/anie.201107557
39. Neugebauer U, Pellegrin Y, Devocelle M, Forster RJ, Signac W, Moran N, Keyes TE (2008) Ruthenium polypyridyl peptide conjugates: membrane permeable probes for cellular imaging. Chem Commun (42):5307–5309
40. Koren K, Borisov SM, Saf R, Klimant I (2011) Strongly phosphorescent iridium(III)–porphyrins—new oxygen indicators with tuneable photophysical properties and functionalities. Eur J Inorgan Chem 2011(10):1531–1534. doi:10.1002/ejic.201100089

41. Stern O, M. Volmer (1919) The fading time of fluorescence. Physikalishe Zeitschrift 20:183–188
42. Becker W, Bergmann A, Biskup C (2007) Multispectral fluorescence lifetime imaging by TCSPC. Microsc Res Tech 70(5):403–409. doi:10.1002/jemt.20432
43. Carraway ER, Demas JN, DeGraff BA, Bacon JR (1991) Photophysics and photochemistry of oxygen sensors based on luminescent transition-metal complexes. Anal Chem 63(4):337–342. doi:10.1021/ac00004a007
44. Schweitzer C, Schmidt R (2003) Physical mechanisms of generation and deactivation of singlet oxygen. Chem Rev 103(5):1685–1758. doi:10.1021/cr010371d
45. Rumsey WL, Vanderkooi JM, Wilson DF (1988) Imaging of phosphorescence: a novel method for measuring oxygen distribution in perfused tissue. Science 241(4873):1649–1651. doi:10.1126/science.3420417
46. Dunphy I, Vinogradov SA, Wilson DF (2002) Oxyphor R2 and G2: phosphors for measuring oxygen by oxygen-dependent quenching of phosphorescence. Anal Biochem 310(2):191–198
47. Lebedev AY, Troxler T, Vinogradov SA (2008) Design of metalloporphyrin-based dendritic nanoprobes for two-photon microscopy of oxygen. J Porphyr Phthalocyanines 12(12):1261–1269. doi:10.1142/S1088424608000649
48. Mistlberger Gn, Koren K, Borisov SM, Klimant I (2010) Magnetically remote-controlled optical sensor spheres for monitoring oxygen or pH. Anal Chem 82(5):2124–2128. doi:10.1021/ac902393u
49. Wang W, Upshaw L, Strong DM, Robertson RP, Reems J (2005) Increased oxygen consumption rates in response to high glucose detected by a novel oxygen biosensor system in non-human primate and human islets. J Endocrinol 185(3):445–455. doi:10.1677/joe.1.06092
50. Schmälzlin E, van Dongen JT, Klimant I, Marmodée B, Steup M, Fisahn J, Geigenberger P, Löhmannsröben H-G (2005) An optical multifrequency phase-modulation method using microbeads for measuring intracellular oxygen concentrations in plants. Biophys J 89(2):1339–1345
51. Molter TW, McQuaide SC, Suchorolski MT, Strovas TJ, Burgess LW, Meldrum DR, Lidstrom ME (2009) A microwell array device capable of measuring single-cell oxygen consumption rates. Sens Actuators B Chem 135(2):678–686
52. Thomas PC, Raghavan SR, Forry SP (2011) Regulating oxygen levels in a microfluidic device. Anal Chem 83(22):8821–8824. doi:10.1021/ac202300g
53. Hynes J, Floyd S, Soini AE, O'Connor R, Papkovsky DB (2003) Fluorescence-based cell viability screening assays using water-soluble oxygen probes. J Biomol Screen 8(3):264–272. doi:10.1177/1087057103008003004
54. Dmitriev RI, Ropiak H, Ponomarev G, Yashunsky DV, Papkovsky DB (2011) Cell-penetrating conjugates of coproporphyrins with oligoarginine peptides: rational design and application to sensing of intracellular O_2. Bioconjug Chem. doi:10.1021/bc200324q
55. Dmitriev RI, Zhdanov AV, Jasionek G, Papkovsky DB (2012) Assessment of cellular oxygen gradients with a panel of phosphorescent oxygen-sensitive probes. Anal Chem 84(6):2930–2938. doi:10.1021/ac3000144
56. Dmitriev RI, Ropiak HM, Yashunsky DV, Ponomarev GV, Zhdanov AV, Papkovsky DB (2010) Bactenecin 7 peptide fragment as a tool for intracellular delivery of a phosphorescent oxygen sensor. FEBS J 277(22):4651–4661. doi:10.1111/j.1742-4658.2010.07872.x
57. Koren K, Dmitriev RI, Borisov SM, Papkovsky DB, Klimant I (2012) Complexes of IrIII-octaethylporphyrin with peptides as probes for sensing cellular O_2. ChemBioChem 13:1184–1190. doi:10.1002/cbic.201200083
58. Koo Lee Y-E, Smith R, Kopelman R (2009) Nanoparticle PEBBLE sensors in live cells and in vivo. Ann Rev Anal Chem 2(1):57–76. doi:10.1146/annurev.anchem.1.031207.112823

59. Koo Lee Y-E, Ulbrich EE, Kim G, Hah H, Strollo C, Fan W, Gurjar R, Koo S, Kopelman R (2010) Near infrared luminescent oxygen nanosensors with nanoparticle matrix tailored sensitivity. Anal Chem 82(20):8446–8455. doi:10.1021/ac1015358
60. Coogan MP, Court JB, Gray VL, Hayes AJ, Lloyd SH, Millet CO, Pope SJA, Lloyd D (2010) Probing intracellular oxygen by quenched phosphorescence lifetimes of nanoparticles containing polyacrylamide-embedded [Ru(dpp(SO3Na)2)3]Cl2. Photochem Photobiol Sci 9(1):103–109
61. Borisov SM, Mayr T, Mistlberger G, Waich K, Koren K, Chojnacki P, Klimant I (2009) Precipitation as a simple and versatile method for preparation of optical nanochemosensors. Talanta 79(5):1322–1330. doi:10.1016/j.talanta.2009.05.041
62. Wu C, Bull B, Christensen K, McNeill J (2009) Ratiometric single-nanoparticle oxygen sensors for biological imaging. Angew Chemie Int Ed 48(15):2741–2745. doi:10.1002/anie.200805894
63. Wang X-d, Gorris HH, Stolwijk JA, Meier RJ, Groegel DBM, Wegener J, Wolfbeis OS (2011) Self-referenced RGB colour imaging of intracellular oxygen. Chem Sci 2(5):901–906
64. Zhdanov AV, Ogurtsov VI, Taylor CT, Papkovsky DB (2010) Monitoring of cell oxygenation and responses to metabolic stimulation by intracellular oxygen sensing technique. Integr Biol 2(9):443–451
65. Golub AS, Barker MC, Pittman RN (2007) PO2 profiles near arterioles and tissue oxygen consumption in rat mesentery. Am J Physiol Heart Circ Physiol 293(2):H1097–H1106. doi:10.1152/ajpheart.00077.2007
66. Golub AS, Pittman RN (2008) PO2 measurements in the microcirculation using phosphorescence quenching microscopy at high magnification. Am J Physiol Heart Circ Physiol 294(6):H2905–H2916. doi:10.1152/ajpheart.01347.2007
67. Golub AS, Tevald MA, Pittman RN (2011) Phosphorescence quenching microrespirometry of skeletal muscle in situ. Am J Physiol Heart Circ Physiol 300(1):H135–H143. doi:10.1152/ajpheart.00626.2010
68. Pittman RN, Golub AS, Carvalho H (2010) Measurement of oxygen in the microcirculation using phosphorescence quenching microscopy. Oxyg Transp Tissue XXXI. In: Takahashi E, Bruley DF (eds) Advances in experimental medicine and biology, vol 662. Springer, US, pp 157–162. doi:10.1007/978-1-4419-1241-1_22
69. Shonat RD, Kight AC (2003) Oxygen tension imaging in the mouse retina. Ann Biomed Eng 31(9):1084–1096. doi:10.1114/1.1603256
70. Lo L-W, Koch CJ, Wilson DF (1996) Calibration of oxygen-dependent quenching of the phosphorescence of Pd-meso-tetra (4-Carboxyphenyl) porphine: a phosphor with general application for measuring oxygen concentration in biological systems. Anal Biochem 236(1):153–160. doi:10.1006/abio.1996.0144
71. Estrada AD, Ponticorvo A, Ford TN, Dunn AK (2008) Microvascular oxygen quantification using two-photon microscopy. Opt Lett 33(10):1038–1040
72. Wilson DF, Vinogradov SA, Grosul P, Sund N, Vacarezza MN, Bennett J (2006) Imaging oxygen pressure in the rodent retina by phosphorescence lifetime. In: Cicco G, Bruley DF, Ferrari M (eds) Advances in experimental medicine and biology, vol 578. Springer, US, pp 119–124. doi:10.1007/0-387-29540-2_19
73. Diepart C, Verrax J, Calderon PB, Feron O, Jordan BF, Gallez B (2010) Comparison of methods for measuring oxygen consumption in tumor cells in vitro. Anal Biochem 396(2):250–256
74. Hynes J, Marroquin LD, Ogurtsov VI, Christiansen KN, Stevens GJ, Papkovsky DB, Will Y (2006) Investigation of drug-induced mitochondrial toxicity using fluorescence-based oxygen-sensitive probes. Toxicol Sci 92(1):186–200. doi:10.1093/toxsci/kfj208
75. Zhdanov AV, Favre C, O'Flaherty L, Adam J, O'Connor R, Pollard PJ, Papkovsky DB (2011) Comparative bioenergetic assessment of transformed cells using a cell energy budget platform. Integr Biol 3(11):1135–1142

76. Sakadzic S, Roussakis E, Yaseen MA, Mandeville ET, Srinivasan VJ, Arai K, Ruvinskaya S, Devor A, Lo EH, Vinogradov SA, Boas DA (2010) Two-photon high-resolution measurement of partial pressure of oxygen in cerebral vasculature and tissue. Nat Meth 7(9):755–759
77. Finikova OS, Lebedev AY, Aprelev A, Troxler T, Gao F, Garnacho C, Muro S, Hochstrasser RM, Vinogradov SA (2008) Oxygen microscopy by two-photon-excited phosphorescence. ChemPhysChem 9(12):1673–1679. doi:10.1002/cphc.200800296
78. Esipova TV, Karagodov A, Miller J, Wilson DF, Busch TM, Vinogradov SA (2011) Two new "protected" oxyphors for biological oximetry: properties and application in tumor imaging. Anal Chem. doi:10.1021/ac2022234
79. Napp J, Behnke T, Fischer L, Würth C, Wottawa M, Katschinski DM, Alves F, Resch-Genger U, Schäferling M (2011) Targeted luminescent near-infrared polymer-nanoprobes for in vivo imaging of tumor hypoxia. Anal Chem. doi:10.1021/ac201870b
80. Zhdanov AV, Ward MW, Taylor CT, Souslova EA, Chudakov DM, Prehn JH, Papkovsky DB (2010) Extracellular calcium depletion transiently elevates oxygen consumption in neurosecretory PC12 cells through activation of mitochondrial Na(+)/Ca(2+) exchange. Biochimica et biophysica acta 1797(9):1627-1637. doi:S0005-2728(10)00629-8[pii]10.1016/j.bbabio.2010.06.006
81. Zhdanov AV, Ward MW, Prehn JHM, Papkovsky DB (2008) Dynamics of intracellular oxygen in PC12 cells upon stimulation of neurotransmission. J Biol Chem 283(9):5650–5661. doi:10.1074/jbc.M706439200
82. O'Riordan TC, Zhdanov AV, Ponomarev GV, Papkovsky DB (2007) Analysis of intracellular oxygen and metabolic responses of mammalian cells by time-resolved fluorometry. Anal Chem 79(24):9414–9419. doi:10.1021/ac701770b
83. Zhdanov A, Dmitriev R, Papkovsky D (2011) Bafilomycin A1 activates respiration of neuronal cells via uncoupling associated with flickering depolarization of mitochondria. Cell Mol Life Sci 68(5):903–917. doi:10.1007/s00018-010-0502-8
84. Koo Y-EL, Cao Y, Kopelman R, Koo SM, Brasuel M, Philbert MA (2004) Real-time measurements of dissolved oxygen inside live cells by organically modified silicate fluorescent nanosensors. Anal Chem 76(9):2498–2505. doi:10.1021/ac035493f
85. Wotzlaw C, Bernardini A, Berchner-Pfannschmidt U, Papkovsky D, Acker H, Fandrey J (2011) Multifocal animated imaging of changes in cellular oxygen and calcium concentrations and membrane potential within the intact adult mouse carotid body ex vivo. Am J Physiol Cell Physiol. doi:10.1152/ajpcell.00508.2010
86. Dmitriev RI, Zhdanov AV, Ponomarev GV, Yashunski DV, Papkovsky DB (2010) Intracellular oxygen-sensitive phosphorescent probes based on cell-penetrating peptides. Anal Biochem 398(1):24–33
87. Fercher A, Borisov SM, Zhdanov AV, Klimant I, Papkovsky DB (2011) Intracellular O_2 sensing probe based on cell-penetrating phosphorescent nanoparticles. ACS Nano 5:5499–5508. doi:10.1021/nn200807g
88. Kondrashina AV, Dmitriev RI, Borisov SM, Klimant I, O'Brian I, Nolan YM, Zhdanov AV, Papkovsky DB (2012) A phosphorescent nanoparticle based probe for sensing and imaging of (intra)cellular oxygen in multiple detection modalities. Adv Funct Mater. doi:10.1002/adfm.201201387
89. Lakowicz JR (2006) Principles of fluorescence Spectroscopy, 3rd ed. Springer, 954 p
90. Periasamy A, Diaspro A (2003) Multiphoton microscopy. J Biomed Opt 8(3):327–328. doi:10.1117/1.1594726
91. Periasamy A, Elangovan M, Elliott E, Brautigan DL (2002) Fluorescence lifetime imaging (FLIM) of green fluorescent fusion proteins in living cells. Methods Mol Biol 183:89–100. doi:10.1385/1-59259-280-5:089
92. Xiang H, Zhou L, Feng Y, Cheng J, Wu D, Zhou X (2012) Tunable fluorescent/phosphorescent platinum(II) porphyrin–fluorene copolymers for ratiometric dual emissive oxygen sensing. Inorgan Chem. doi:10.1021/ic300040n

93. Tsai AG, Friesenecker B, Mazzoni MC, Kerger H, Buerk DG, Johnson PC, Intaglietta M (1998) Microvascular and tissue oxygen gradients in the rat mesentery. Proc Natl Acad Sci 95(12):6590–6595
94. Fercher A, O'Riordan TC, Zhdanov AV, Dmitriev RI, Papkovsky DB (2010) Imaging of cellular oxygen and analysis of metabolic responses of mammalian cells. Methods Mol Biol 591:257–273. doi:10.1007/978-1-60761-404-3_16
95. Becker W, Su B, Holub O, weisshart K (2010) FLIM and FCS detection in laser-scanning microscopes: Increased efficiency by GaAsP hybrid detectors. Microsc Res Tech 74(9):804–811. doi:10.1002/jemt.20959
96. Will Y, Hynes J, Ogurtsov VI, Papkovsky DB (2006) Analysis of mitochondrial function using phosphorescent oxygen-sensitive probes. Nat Protoc 1(6):2563–2572. doi:nprot.2006.351[pii]10.1038/nprot.2006.351
97. Zitova A, Hynes J, Kollar J, Borisov SM, Klimant I, Papkovsky DB (2010) Analysis of activity and inhibition of oxygen-dependent enzymes by optical respirometry on the LightCycler system. Anal Biochem 397(2):144–151
98. Papkovsky DB, O'Riordan T, Soini A (2000) Phosphorescent porphyrin probes in biosensors and sensitive bioassays. Biochem Soc Trans 28(2):74–77
99. O'Mahony FC, Papkovsky DB (2006) Rapid high-throughput assessment of aerobic bacteria in complex samples by fluorescence-based oxygen respirometry. Appl Environ Microbiol 72(2):1279–1287. doi:10.1128/aem.72.2.1279-1287.2006
100. O'Flaherty L, Adam J, Heather LC, Zhdanov AV, Chung YL, Miranda MX, Croft J, Olpin S, Clarke K, Pugh CW, Griffiths J, Papkovsky D, Ashrafian H, Ratcliffe PJ, Pollard PJ (2010) Dysregulation of hypoxia pathways in fumarate hydratase-deficient cells is independent of defective mitochondrial metabolism. Hum Mol Genet 19(19):3844–3851. doi:ddq305 [pii] 10.1093/hmg/ddq305
101. O'Hagan KA, Cocchiglia S, Zhdanov AV, Tambuwala MM, Cummins EP, Monfared M, Agbor TA, Garvey JF, Papkovsky DB, Taylor CT, Allan BB (2009) PGC-1alpha is coupled to HIF-1alpha-dependent gene expression by increasing mitochondrial oxygen consumption in skeletal muscle cells. Proc Natl Acad Sci U S A 106(7):2188–2193. doi:0808801106 [pii] 10.1073/pnas.0808801106
102. Frezza C, Zheng L, Tennant DA, Papkovsky DB, Hedley BA, Kalna G, Watson DG, Gottlieb E (2011) Metabolic profiling of hypoxic cells revealed a catabolic signature required for cell survival. PLoS ONE 6(9):e24411. doi:10.1371/journal.pone.0024411
103. Semenza GL (2010) Oxygen homeostasis. Wiley Interdiscip Rev Sys BiolMed 2(3):336–361. doi:10.1002/wsbm.69
104. Wong C, Zhang H, Gilkes D, Chen J, Wei H, Chaturvedi P, Hubbi M, Semenza G (2012) Inhibitors of hypoxia-inducible factor 1 block breast cancer metastatic niche formation and lung metastasis. J Mol Med 90:803–815. doi:10.1007/s00109-011-0855-y
105. Ferrick DA, Neilson A, Beeson C (2008) Advances in measuring cellular bioenergetics using extracellular flux. Drug Discov Today 13(5–6):268–274. doi:10.1016/j.drudis.2007.12.008
106. Huppert TJ, Allen MS, Benav H, Jones PB, Boas DA (2007) A multicompartment vascular model for inferring baseline and functional changes in cerebral oxygen metabolism and arterial dilation. J Cereb Blood Flow Metab Off J Int Soc Cereb Blood Flow Metab 27(6):1262–1279
107. Fang Q, Sakadzic S, Ruvinskaya L, Devor A, Dale AM, Boas DA (2008) Oxygen advection and diffusion in a three- dimensional vascular anatomical network. Opt Express 16(22):17530–17541
108. Zheng L, Golub AS, Pittman RN (1996) Determination of PO2 and its heterogeneity in single capillaries. Am J Physiol Heart Circ Physiol 271(1):H365–H372
109. Yaseen MA, Srinivasan VJ, Sakadzic S, Wu W, Ruvinskaya S, Vinogradov SA, Boas DA (2009) Optical monitoring of oxygen tension in cortical microvessels with confocal microscopy. Opt Express 17(25):22341–22350. doi:10.1364/OE.17.022341190652 [pii]

110. Howlett RA, Kindig CA, Hogan MC (2007) Intracellular PO2 kinetics at different contraction frequencies in Xenopus single skeletal muscle fibers. J Appl Physiol 102(4):1456–1461. doi:10.1152/japplphysiol.00422.2006
111. Zhang S, Hosaka M, Yoshihara T, Negishi K, Iida Y, Tobita S, Takeuchi T (2010) Phosphorescent lightâ€“emitting iridium complexes serve as a hypoxia-sensing probe for tumor imaging in living animals. Can Res 70(11):4490–4498. doi:10.1158/0008-5472.can-09-3948
112. Robiolio M, Rumsey WL, Wilson DF (1989) Oxygen diffusion and mitochondrial respiration in neuroblastoma cells. Am J Physiol Cell Physiol 256(6):C1207–C1213
113. Mik EG, Ince C, Eerbeek O, Heinen A, Stap J, Hooibrink B, Schumacher CA, Balestra GM, Johannes T, Beek JF, Nieuwenhuis AF, van Horssen P, Spaan JA, Zuurbier CJ (2009) Mitochondrial oxygen tension within the heart. J Mol Cell Cardiol 46(6):943–951
114. van Dongen JT, Gupta KJ, Ramírez-Aguilar SJ, Araújo WL, Nunes-Nesi A, Fernie AR (2011) Regulation of respiration in plants: A role for alternative metabolic pathways. J Plant Physiol 168(12):1434–1443
115. Zitova A, O'Mahony FC, Cross M, Davenport J, Papkovsky DB (2009) Toxicological profiling of chemical and environmental samples using panels of test organisms and optical oxygen respirometry. Environ Toxicol 24(2):116–127. doi:10.1002/tox.20387
116. Lo JF, Wang Y, Blake A, Yu G, Harvat TA, Jeon H, Oberholzer J, Eddington DT (2012) Islet preconditioning via multimodal microfluidic modulation of intermittent hypoxia. Anal Chem 84(4):1987–1993. doi:10.1021/ac2030909